Molecular basis for the inhibition of 1,4-dihydropyridine calcium channel drugs binding to their receptors by a nonspecific site interaction mechanism

Howard S. Young,*,¶ Victor Skita,§,¶ R. Preston Mason,§,¶ and Leo G. Herbette*,‡,§,¶
Departments of *Biochemistry, ‡Medicine and §Radiology, and ¶Biomolecular Structure Analysis Center, University of Connecticut Health Center, Farmington, Connecticut 06030-2017

ABSTRACT The "membrane bilayer" pathway (Rhodes, D. G., J. G. Sarmiento, and L. G. Herbette. 1985. *Mol. Pharmacol.* 27:612–623.) for 1,4-dihydropyridine calcium channel drug (DHP) binding to receptor sites in cardiac sarcolemmal membranes has been extended to include the interaction of amphiphiles within the lipid bilayer. These studies focused on the ability of the Class III antiarrhythmic agents bretylium and clofilium to nonspecifically inhibit DHP-receptor binding in canine cardiac sarcolemma. Clofilium was found to inhibit nimodipine binding with an inhibition constant of ~5 μM, whereas bretylium had no effect on nimodipine binding. Small angle x-ray diffraction was then used to examine the differential ability of these two Class III agents to inhibit DHP-receptor binding. The time-averaged locations of bretylium, clofilium, and nimodipine in bovine cardiac phosphatidylcholine (BCPC) bilayers (supplemented with 13 mol% cholesterol) were determined to a resolution of 9 Å. The location of bretylium as dominated by its phenyl ring in BCPC bilayers was found to be at the hydrocarbon core/water interface, similar to that of the dihydropyridine ring of nimodipine. The location of clofilium as dominated by its phenyl ring was found to be below the hydrocarbon/core water interface within the hydrocarbon chain region of the bilayer, similar to that of the phenyl ring of nimodipine. The location of the dihydropyridine ring portion of nimodipine has previously been shown by neutron diffraction to be located at the hydrocarbon core/water interface of native sarcoplasmic reticulum, consistent with the small angle x-ray data from model membranes in this paper. Therefore, we speculate that the nonspecific inhibition arises from the interaction of clofilium's phenyl ring with the site on the calcium channel receptor where the phenyl ring portion of nimodipine must interact. The DHP-receptor binding pathway would then involve both nonspecific (membrane) and specific (protein) binding components, both of which are necessary for receptor binding.

INTRODUCTION

1,4-dihydropyridine calcium channel agonists and antagonists (DHPs) are a class of similar chemicals that reversibly modulate cardiac and smooth muscle excitation-contraction coupling mechanisms (for review see Janis et al., 1987). Despite the important clinical role of DHPs, the mechanistic basis for their action on cellular calcium flux has yet to be fully characterized. Since the recent review of this subject (Mason et al., 1990), our understanding of the DHP-receptor binding pathway has been refined and extended, principally through studies of the interactions of cardiac drugs with biological membranes.

DHPs inhibit voltage-sensitive calcium channels in cardiac sarcolemma in a highly stereoselective, saturable and reversible manner (Belleman et al., 1983). Equilibrium dissociation constants for the interaction of DHPs with receptors in cardiac, smooth and skeletal muscle are in the range of 0.1 to 5 nM. These molecules are also generally lipophilic and partition nonspecifically with relatively high partition coefficients into model and native membranes (Herbette et al., 1986). This lipophilicity often correlates with electrophysiological effects (Kokubun and Reuter, 1984), suggesting that this property is directly involved in its mechanism of action.

These and other observations have led to the formulation of a "membrane bilayer pathway" describing the mechanism of DHP-receptor binding (Rhodes et al., 1985). A general hydrophobic pathway has also been proposed to address receptor binding for other amphiphilic drugs, such as local anesthetics (Hille, 1977), general anesthetics (for review see Franks and Lieb, 1987), barbituates (Miller and Roth, 1986), benzodiazepines (for review see Herbette et al., 1991), cannabinoids (for review see Martin, 1986), and others. The membrane bilayer pathway of Rhodes et al. (1985) involves drug partitioning to an energy favorable location in the bilayer followed by lateral diffusion to its protein receptor site. A substantial kinetic advantage is gained by the bilayer pathway (versus a diffusion-limited aqueous approach) in biological membranes where the receptor site density is low (McCloskey and Poo, 1986) and for DHPs with high partition coefficients for the membrane bilayer (Herbette et al., 1986). Experimental support for this pathway exists in the form of studies of the lateral diffusion of DHPs in membranes (Chester et

Address correspondence to Dr. Herbette.

0006-3495/92/05/1244/12 $2.00

al., 1987), receptor binding studies (Affolter and Coronado, 1985; Valdivia and Coronado, 1988), and electrophysiological studies (Kokubun and Reuter, 1984). The proposed membrane bilayer pathway model links nonspecific DHP-membrane interactions, as described above, with specific binding to a stereoselective, saturable and reversible high affinity protein receptor site.

To further investigate interactions of DHPs with both the membrane bilayer and their target protein receptor, we have recently examined the ability of other lipid soluble drugs to inhibit the binding of nimodipine to its high affinity receptor site. Bretylium is a Class III antiarrhythmic drug which is potentially useful in terminating abnormal cardiac rhythms (Steinberg, 1988). A diverse group of compounds possess Class III activity including bretylium, clofilium and amiodarone, which share the property of being amphiphilic molecules containing halogenated phenyl moieties. Proposed ionic mechanisms for Class III activity include effects on inward sodium currents, calcium influx, and outward potassium currents, although at least for amiodarone a specific receptor is not believed to exist. In this study, the molecular basis for the differential ability of bretylium and clofilium to inhibit DHP-receptor binding in canine cardiac sarcolemmal membranes was addressed. Small angle x-ray diffraction was used to determine the time-averaged location of the Class III antiarrhythmic agents clofilium and bretylium (in addition to that of nimodipine) in the membrane bilayer and these locations were compared with the ability of these agents to nonspecifically inhibit nimodipine's binding to its receptor.

METHODS AND MATERIALS

Chemicals

Bretylium was a gift from American Hospital Supply Corp. (McGaw Park, IL). Clofilium was a gift of Eli Lily and Co. (Indianapolis, IN). Nimodipine was a gift of Miles Pharmaceuticals, a Division of Miles Laboratories (West Haven, CT). The drugs were dissolved in 100% ethanol due to their limited aqueous solubility, and stored at 0°C. Bovine cardiac phosphatidylcholine (BCPC) was purchased from Avanti Polar-Lipid, Inc. (Birmingham, AL), and stored in powdered form at 0°C. Lipid purity and integrity was assessed, before and after x-ray diffraction studies, to be >95% phosphatidylcholine by thin-layer chromatography. All other chemicals were reagent grade and all solutions were made using glass distilled deionized water.

Competition binding analysis

Crude canine cardiac sarcolemmal (CSL) membranes were isolated by the method of Jones et al. (1980).

150 nM ^{3}H-nimodipine and varying concentrations of either bretylium or clofilium were incubated with 150 μg of CSL membranes in a final volume of 495 μl, at 25°C for 90 min. The reaction mixtures were then rapidly filtered through GF-C filters pretreated with 0.3% polyethylenimine, and washed with four volumes (2.5 ml) of buffer (50 mM Tris-HCl, pH 7.4). The radioactivity remaining in the membranes on the filters was then determined by scintillation counting.

The bretylium and clofilium concentration range used for the competition binding assays was 3 nM to 500 μM. Control experiments were performed competing nonradiolabeled nimodipine against ^{3}H-nimodipine. These experiments utilized fixed concentrations of 150 nM ^{3}H-nimodipine against varying concentrations of nimodipine, ranging from 0.05 to 300 nM. Nonspecific binding was determined by competing 150 nM ^{3}H-nimodipine against saturating concentrations (50 μM) of nimodipine. All competition binding values were corrected for nonspecific binding.

The values were expressed as percent of total counts per minute. Total cpms were determined by counting CSL membranes in the presence of 150 nM ^{3}H-nimodipine and no drug. Three data points were determined for each concentration (n = 3). Inhibition constants (K_i) were determined as the concentration of drug necessary for half-maximal inhibition of ^{3}H-nimodipine binding.

Preparation of multibilayer samples for x-ray diffraction

The phospholipid composition of the CSL membranes was previously determined to be primarily phosphatidylcholine (45%) and phosphatidylethanolamine (36%) with lesser amounts of phosphatidylserine and sphingomyelin (8%), phosphatidylinositol (7%), and phosphatidylglycerol (1%); cholesterol accounted for ~13 mol% of the phospholipid content (Mason et al., 1989). As a model system, we used a source of BCPC supplemented with 13 mol% cholesterol.

BCPC multilamellar lipid vesicles were prepared in the absence or presence of known amounts of bretylium, clofilium, or nimodipine essentially by the method of Bangham et al. (1965). BCPC multilamellar vesicles were prepared as follows: the desired amount of lipid and the desired amount of cholesterol dissolved in $CHCl_3$ were placed in a glass test tube and dried down to a thin film under vacuum. Buffer (0.5 mM Hepes, 2.0 mM NaCl, pH 7.27), in the presence and absence of known bretylium, clofilium, or nimodipine concentrations, was added to yield a final lipid concentration of 5 mg/ml and a drug-to-lipid ratio of 1:30. This solution was then vortexed and sonicated to form a cloudy white suspension of multilamellar vesicles. The membrane samples were stored at 4°C.

Multibilayer samples for small angle x-ray diffraction were prepared as described previously (Chester et al., 1987). Sample preparation and dehydration took ~3 h; this ensures sufficient time, based on our kinetic measurements, for drug partitioning into the membrane to reach equilibrium.

The salts used for controlling relative humidity (r.h.) were LiCl, 13%; $MgCl_2$, 34%; K_2CO_3, 45%; $Mg(NO_3)_2$, 55%; $NaNO_3$, 66%; K_2tartarate, 72%; $(NH_4)_2SO_4$, 81%; Na/Ktartarate, 87%; and $ZnSO_4$, 93%.

Small angle x-ray diffraction

CuK x-rays produced by a GX-18 rotating anode generator (Enraf Nonius, Bohemia, NY) were either line focused for the small angle studies or point focused for the equatorial studies using Franks' mirror assemblies. A nickel filter was used to select CuK_α radiation (λ = 1.54 Å).

Diffraction data collection

Data was recorded on a Braun position sensitive 1-dimensional detector (Innovative Technologies, Inc., South Hamilton, MA) interfaced to a MicroVax II (Digital Equip. Corp., Maynard, MA).

Data reduction (background and geometrical corrections) has been

described previously (Herbette et al., 1985). Briefly, an exponential function was fit to the background and subtracted in the integration routine. Since the entire lamellar reflection for each observed intensity was collected by the detector, the lamellar intensity functions from the BCPC samples collected with the electronic detector were simply Lorentz corrected by a factor of $s = 2 \sin \Theta/\lambda$.

Data were recorded on Kodak DEF-5 (Eastman Kodak Co., Rochester, NY) film and qualitatively examined to determine the high angle acyl-chain packing of the samples and to verify the low angle detector data.

Phasing the data

A swelling analysis was used to phase the lamellar reflections for each experiment (Moody, 1963). Eight sets of intensity data obtained at different hydration states ranging from 93 to 13% r.h., each with unique unit cell repeat distances, were used to assign an unambiguous phase combination to the experimentally obtained structure factors (h = 1–4). Due to insufficient data, the shape of the structure factor function in the region of $h = 5$ and $h = 6$ could not be ascertained. The possible phase combinations were further refined to a single solution using the "swellcheck" analysis described below. This phase combination was confirmed through the autocorrelation analysis. The final phase choice was the only physically reasonable combination, in terms of empirical examination of resultant electron density profiles.

Swellcheck analysis

The swelling series utilized in the experiments ranged from 93 to 13% r.h. The electron density profile at each humidity was calculated as the symmetric Fourier transform of the square root of the Lorentz-corrected, integrated intensity function along with the corresponding phase information. The resultant electron density profiles were inverse Fourier transformed to obtain the continuous structure factor function, F(s), at each hydration state. The resultant structure factors were sampled at integer multiples of the reciprocal unit cell repeat distances, $1/d$, obtained for the entire swelling series and then Fourier transformed to reconstruct the experimental electron density profiles, $\rho(x)$ (Shannon, 1949; Sayre, 1953). The reconstructed electron density profiles, $\rho_r(x)$, corresponding to the repeat distance at each humidity, were compared to the corresponding experimental electron density profiles, $\rho_{ex}(x)$. Assuming the structure is conserved at the hydration states used to construct the structure factor, then $\rho_r(x)$ for a given repeat distance should be identical to, within experimental error, the $\rho_{ex}(x)$ at that same relative humidity. This analysis tests the validity of the assumption used in the swelling analysis. The swellcheck analysis also provides a quantitative error analysis, presented in the form of a calculated residual (as described below). The errors reflected in this residual include experimental error in sample variation and data collection, deviation of the sample from the assumption of the swelling analysis, and error in the data analysis.

Demanding consistency in the swellcheck analysis aided in unambiguously verifying the phase combination chosen for the structure factors and in eliminating the remaining ambiguous phase combinations.

Autocorrelation analysis

The multilayer autocorrelation function, $P_{ml}(x)$, was calculated as the Fourier transformation of the corrected intensities placed at the corresponding h/d values. A difference-$P_{ml}(x)$, $\Delta P_{ml}(x)$, was calculated as the normalized drug-$P_{ml}(x)$, $P_{dml}(x)$, minus the normalized control-$P_{ml}(x)$, $P_{cml}(x)$. Assuming the isomorphic addition of the drug to the membrane bilayer, the difference-autocorrelation function can be interpreted to directly yield the position of the drug molecule in the membrane. Details of this method can be found in the Appendix.

RESULTS

The structural formulas of the Class III antiarrhythmic agents bretylium and clofilium and the DHP nimodipine are shown in Fig. 1.

Competition binding analysis

Bretylium, in the concentration range of 3 nM to 500 μM, did not inhibit nimodipine binding to the DHP receptor in crude CSL membranes. At 500 μM bretylium competing against 150 nM ^{3}H-nimodipine, 100% of the radiolabeled DHP remains bound to its high affinity receptor site (n = 3). Clofilium, however, displaces 90% of the ^{3}H-nimodipine at a concentration of 150 μM (Fig. 2). Another Class III antiarrhythmic agent, amiodarone, gave a similar inhibition effect as that observed with clofilium (data not shown).

The K_i value for clofilium is ~5 μM, whereas bretylium does not inhibit nimodipine binding to CSL membranes. The K_i value determined for nimodipine competed against itself is ~0.5 nM.

Small angle x-ray diffraction studies

The swelling series ranged from 93 to 13% r.h. for both drug-containing and control BCPC samples. The unique phase combination proved to be correct for the following reasons: (a) a $F(s)$ with an unreasonable phase combina-

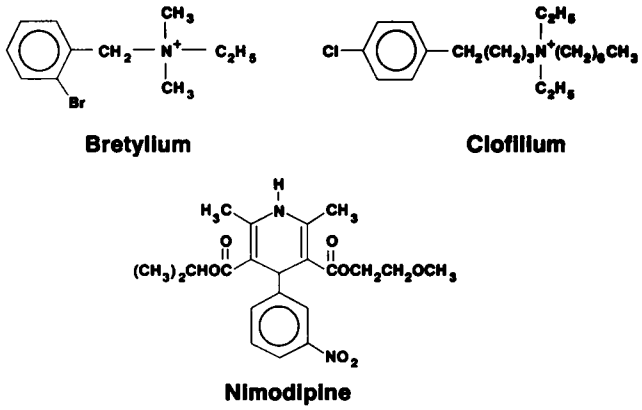

FIGURE 1 The structural formulas for the three drugs used in these studies. Bretylium and clofilium are Class III antiarrhythmic agents which appear to possess similar mechanisms of action. The 1,4-dihydropyridine, nimodipine, is a calcium channel antagonist possessing binding affinity specific for the L-type calcium channel receptor of cardiac sarcolemmal membranes.

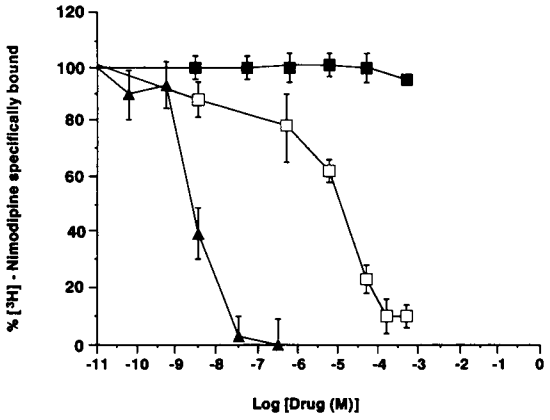

FIGURE 2 Nonspecific inhibition of nimodipine binding by bretylium (*filled squares*), clofilium (*open squares*), and nimodipine (*triangles*). 150 nM of ^{3}H-nimodipine is competed against varying concentrations of bretylium, clofilium or nimodipine, for binding to receptor sites in crude canine cardiac sarcolemmal membranes. The displacement of radiolabeled nimodipine from the membranes reflects inhibition by the competing compound and is calculated as the percent of total counts per minute remaining in the membranes. The K_i value is calculated as the concentration of drug necessary for half-maximal inhibition of nimodipine binding.

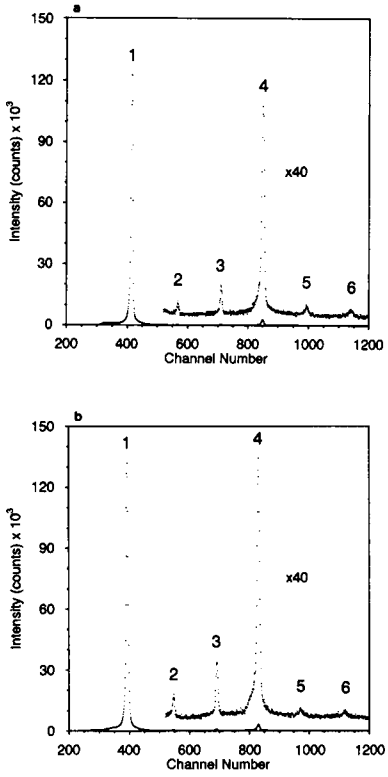

FIGURE 3 X-ray diffraction patterns from BCPC multibilayers in the (*a*) absence and (*b*) presence of bretylium at 55% relative humidity and 6°C collected on a one-dimensional position sensitive x-ray detector. Six sharp lamellar diffraction orders were observed which index at reciprocal vectors of 1/59.2 Å^{-1} and 1/59.0 Å^{-1}, respectively. These diffraction patterns are representative of the type of diffraction data observed in the described experiments.

tion failed to reconstruct the $\rho_{ex}(x)$ in the swellcheck analysis, when sampled at the appropriate d-space and Fourier transformed; (*b*) the $\Delta P_{ml}(x)$, which is phase independent[1], must be consistent with the experimental difference-electron density profile, $\Delta\rho(x)$.

Equatorial diffraction was examined to address the possibility of major structural changes caused by the presence of drug at a 1:30 drug-to-lipid ratio. Acyl-chain packing, indicated by a single, very broad reflection at 1/4.7 Å^{-1}, for both control and drug-containing samples, was found not to be significantly different.

Membrane multibilayers prepared in the presence and absence of bretylium, clofilium, or nimodipine gave clearly defined, reproducible diffraction patterns. The highest resolution diffraction patterns were obtained at a bilayer hydration of 55% and temperatures of 5–10°C. At 55% r.h. and 6°C, for example, we observed six sharp lamellar diffraction orders with an average unit cell repeat distance, d, of 57 Å for a resolution ~9 Å (Fig. 3 and Table 1).

The bretylium-containing BCPC sample and its matched control at 55% r.h. had similar repeat distances of 59.0 and 59.2 Å, respectively. The clofilium-containing sample and its matched control had similar repeat distances of 54.5 and 55.0 Å, respectively. The nimodipine-containing sample and its matched control had repeat distances of 55.9 and 56.3 Å, respectively. In each case, reproducible and localized differences were observed between control and drug-containing samples, which were attributed to the presence of drug. Each drug-containing multibilayer and its matched control is a representative sample selected from at least four identical multilayers, where all the samples in a series had the same lyotropic history. The lyotropic progression for each series was optimized for diffraction quality for the drug-containing samples. Because different lyotropic progressions gave optimal diffraction for the different drug-containing samples, the lyotropic history, and subsequently $F(h)$ for the controls are not the same. The BCPC lipids, in our hands, were found to be very sensitive to the lyotropic progression.

All calculated electron density profiles exhibit characteristics of phospholipid membrane bilayers. A relatively

[1]Since we calculated the control or drug-containing $P_{ml}(x)$ using the sampling theorem, our ΔP_{nl} (x) is not truly phase independent. However, because our d-spaces differed by <0.5 Å in all cases, deviations in the structure factor modulus at the sampled d-spaces are within our 5.1% experimental error.

TABLE 1 **Structure factors evaluated at h/d for BPC in the presence and absence of drug molecules**

h	$F(h)_{control}$	$F(h)_{clofilium}$
1	−0.9399	−0.9473
2	−0.0700	−0.0622
3	+0.1350	+0.1094
4	−0.2934	−0.2766
5	+0.0636	+0.0702
6	−0.0577	−0.0726
	d = 55.0 Å	d = 54.5 Å
h	$F(h)_{control}$	$F(h)_{nimodipine}$
1	−0.8312	−0.8480
2	−0.2772	−0.2768
3	+0.2818	+0.2623
4	−0.3906	−0.3672
5	+0.0124	+0.0055
6	−0.0053	−0.0244
	d = 56.3 Å	d = 55.9 Å
h	$F(h)_{control}$	$F(h)_{bretylium}$
1	−0.9087	−0.9069
2	−0.0402	−0.0586
3	+0.0945	+0.1232
4	−0.3651	−0.3719
5	+0.1262	+0.0948
6	−0.1199	−0.1080
	d = 59.2 Å	d = 59.0 Å

The average experimental error was determined to be 5.1% from the swellcheck analysis.

electron deficient methyl trough is observed at 0 Å, an electron dense headgroup region is observed at ± 22 Å, an acyl chain region is observed between |8 Å| and |18 Å|, and a water-space is observed at $\pm d/2$.

In the swellcheck analysis, the $\rho_r(x)s$ were compared to the experimental profiles of the BCPC multibilayer controls at 55% r.h. The deviation of the $\rho_r(x)$ from the $\rho_{ex}(x)$ represents the experimental error inherent in the electron density profiles. Residuals were calculated, for the reconstruction of the $\rho_{ex}(x)s$, as

$$R = \Sigma[|\rho_{ex}(x) - \rho_r(x)|/|\rho_{ex}(x)|].$$

The average residual for the swellcheck reconstruction was evaluated to be R = 0.051 for $|x| \leq d/2$. This indicates a cumulative error of 5.1% inherent in the $\rho(x)s$, which is consistent with previous error analyses performed in our laboratory (Mason et al., 1989).

In the presence of clofilium, an increase in electron density centered at ±13 Å from the hydrocarbon core center was observed with a distribution of 9 Å ≤ $|x|$ ≤ 16 Å (Fig. 4 *a*). In the presence of nimodipine, an increase in electron density centered at ±16 Å from the hydrocarbon core center was observed, with a distribution of 9 Å ≤ $|x|$ ≤ 22 Å (Fig. 4 *b*). In the presence of bretylium, an increase in electron density was observed centered at ±19 Å from the hydrocarbon core center, superimposing on the phospholipid headgroup/glycerol backbone region of the BCPC bilayer, with a distribution ranging from 14 Å ≤ $|x|$ ≤ 23 Å (Fig. 4 *c*). It is interesting that the extent of electron density distribution changes for nimodipine-containing samples completely overlaps the distributions of bretylium and clofilium, whereas the distributions of bretylium and clofilium do not overlap. The possible implications of this result will be considered in the discussion.

To evaluate the significance of a feature or perturbation in the drug-containing $\rho(x)$, a "degree of significance,"

$$S = \Sigma[|\rho_d(x) - \rho_c(x)|/|\rho_d(x)|],$$

was calculated for drug-containing, $\rho_d(x)$, and control, $\rho_c(x)$, electron density profiles. For the bretylium-control $\rho(x)s$, S = 0.094 for 14 Å ≤ $|x|$ ≤ 23 Å, for the clofilium-control $\rho(x)s$, S = 0.071 for 9 Å ≤ $|x|$ ≤ 16 Å, and for the nimodipine-control $\rho(x)s$, S = 0.136 for 9 Å ≤ $|x|$ ≤ 22 Å. Corresponding residuals for the swellcheck reconstruction of the same regions as that evaluated for the drug-control $\rho(x)s$; R = 0.045 for 14 Å ≤ $|x|$ ≤ 23 Å, R = 0.055 for 9 Å ≤ $|x|$ ≤ 16 Å, and R = 0.036 for 9 Å ≤ $|x|$ ≤ 22 Å. These regions correspond to the headgroup/glycerol backbone region, the acyl-chain region, and the glycerol backbone and acyl chain region of the membrane, respectively. Each residual or significance is the average calculated from $n \geq 4$. In all cases, our degree of significance for the drug-containing samples were higher than the residuals calculated for the same regions of the control electron density profiles.

Autocorrelation analysis

There are two unknowns in the calculation of an absolute electron density profile, the instrumental scaling factor, K, and $F(0)$. Because our $F(s)$ are relative, the electron density profiles can be fit to any data set $KF(s)$, where K is an unknown. The effect of K on the interpretation of electron density profiles is a scaling factor and the effect of $F(0)$ is a constant offset. These two variables complicate the choice of an arbitrary relative scale when comparing electron density profiles.

To direct the choice of K and $F(0)$, autocorrelation analysis of the experimental intensity functions was performed. The $\Delta P_{ml}(x)$ are relatively insensitive to K, as long as K is similar for both data sets. Given that the beam optics, x-ray flux, sample alignment, and detector are virtually the same from one experiment to the next,

FIGURE 4 (*a*) Calculated electron density profiles for clofilium (----) and a matched control (——). The unit cell repeat distances are 54.5 Å and 55.0 Å, respectively, at 55% r.h. and 6°C. The $\Delta\rho(x)$ is shown (– – –), and the electron density difference centered at ±13 Å, with a distribution ranging from |9| to |16| Å, is attributed to the presence of clofilium. α is indicated by the arrow. The $\rho(x)s$ have been minimally scaled and offset such that the $\Delta\rho(x)$ is consistent with the autocorrelation analysis. (*b*) Calculated electron density profiles for nimodipine (----) and a matched control (——). The unit cell repeat distances are 55.9 Å and 56.3Å, respectively, at 55% r.h. and 6°C. The $\Delta\rho(x)$ is shown (– – –), and the electron density difference centered at ±16 Å, with a distribution ranging from |9| to |22| Å, is attributed to the presence of nimodipine. α is indicated by the arrow. The $\rho(x)s$ have been minimally scaled and offset such that the $\Delta\rho(x)$ is consistent with the autocorrelation analysis. (*c*) Calculated electron density profiles for bretylium (----) and a matched control (——). The unit cell repeat distances are 59.0 Å and 59.2 Å, respectively, at 55% r.h. and 6°C. The $\Delta\rho(x)$ is shown (– – –), and the electron density difference centered at ±19 Å, with a distribution ranging from |14 Å| to |23 Å|, is attributed to the presence of bretylium. α and α_1 are indicated by the arrows. The $\rho(x)s$ have been minimally scaled and offset such that the $\Delta\rho(x)$ is consistent with the autocorrelation analysis.

this assumption is valid. $F(0)$ is a function of the number of electrons contributing to the coherent scatter; given the ratio of lipid to drug molecules in our samples, $F(0)$ should vary from 0.5 to 1.7%. Because we are only interested in the location of minima and maxima in the $\Delta P_{ml}(x)$, the effects of $F(0)$ and K are minimized.

The $P_{ml,N}(x)$ (see Appendix), and therefore the $\Delta P_{ml}(x)$, repeats at intervals of d and is centrosymmetric around odd intervals of $d/2$. Consequently, the $\Delta P_{ml}(x)$, need only be considered from zero to $d/2$. For our interpretation, we need only consider the positions of local minima and maxima in the difference-autocorrelation function. Assuming the "isomorphous" addition of drug to the membrane bilayer, the positions of the minima and maxima allows us to deduce the location of the "isomorph" in the bilayer structure.[2] This difference-autocorrelation is to the same inherent resolution as the electron density profiles. Scale factors and $F(0)$ affect the magnitudes of the minima and maxima in the $\Delta P_{ml}(x)$, but otherwise have little effect on its interpretation. The greater the divergence from isomorphism, the more complicated the interpretation of the $\Delta P_{ml}(x)$ becomes. This is exemplified by the bretylium data set where the need to consider a more complicated model arises. The maxima and minima in the $\Delta P_{ml}(x)$ appear shifted from the locations predicted by the $\rho(x)s$. These shifts are predicted theoretically and will be discussed in a future paper.

[2]By isomorph, we mean a single perturbation to the bilayer structure. In our case, this includes the additional electron density contributed by the presence of drug molecules and/or changes in the bilayer structure caused by the presence of drug molecules.

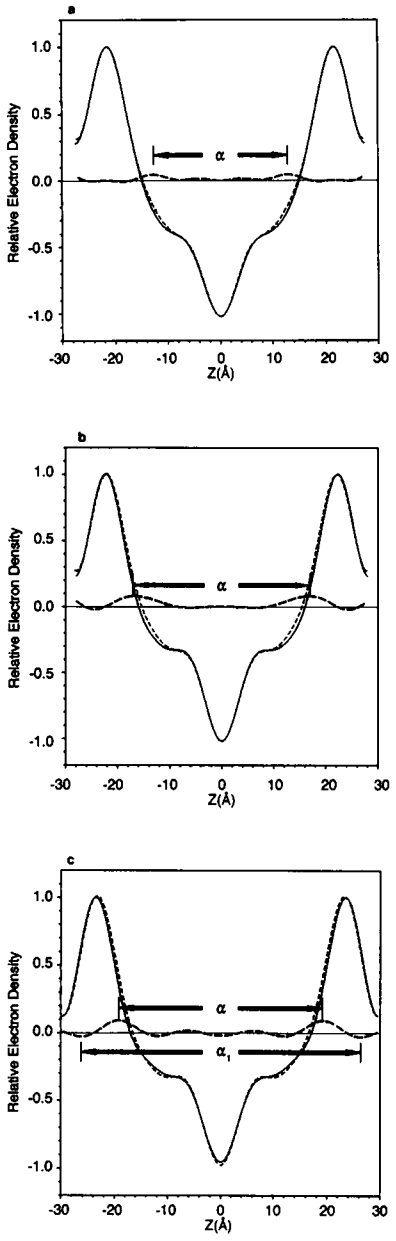

Fig. 5 shows two unit cells of the nimodipine-containing and control $\rho(x)s$, with the significant autocorrelations one observes in the calculated $\Delta P_{ml}(x)$. These features in the autocorrelation function arise from the presence of the isomorph. Similar features are observed in the case of clofilium and bretylium.

The $\Delta P_{ml}(x)$, calculated for the clofilium versus control $P_{ml,N}(x)s$ (Fig. 6 *a*), indicated a maximum at 8 Å, a minimum at 14 Å and a second maximum at 21 Å. The maximum at 8 Å corresponds to the headgroup-isomorph autocorrelation, the minimum at 14 Å corresponds to the isomorph-methyl trough autocorrelation, and the maximum at 21 Å corresponds to the autocorre-

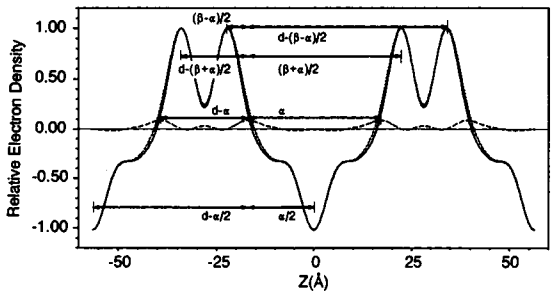

FIGURE 5 Interpretation of the difference-autocorrelation function, illustrated for the nimodipine data set. Two unit cells for the control (——) and nimodipine-containing (----) BCPC bilayers are shown. The $\Delta\rho(x)$ is also shown (– – –). The vertical lines at ±16 Å indicate the nimodipine location in each monolayer. The arrows indicate the major autocorrelations predicted for the $\Delta P_{ml}(x)$, in the range of zero to d. β is the distance between headgroup maxima in the unit cell, and α is the distance between isomorph (i.e., drug) maxima in the unit cell. $(\beta - \alpha)/2$ is the autocorrelation between the isomorph and the nearest headgroup. $(\beta + \alpha)/2$ is the autocorrelation between the isomorph and the opposite headgroup in the unit cell. α is the autocorrelation between isomorphs in the unit cell. $\alpha/2$ is the autocorrelation between the isomorph and the methyl-trough region of the unit cell. Autocorrelations with the adjacent unit cell are also predicted and are shown in the figure.

lation of the isomorph with the nearest headgroup in the adjacent unit cell of the multibilayer (See Fig. 5 and Appendix). There are other autocorrelations at 4 Å and $d/2$ which, based on model calculations, are explained by the addition of a small perturbation to the water-space. The electron density increase attributed to the presence of clofilium would then be located at ~14 Å from the methyl-trough of the BCPC bilayer.

The $\Delta P_{ml}(x)$, calculated from the nimodipine versus control $P_{ml,N}(x)s$ (Figs. 5 and 6 *b* for interpretation), indicated a maximum at 6 Å, a minimum at 14 Å and a second maximum at 20 Å. The interpretation of these minima and maxima is similar to that described above for clofilium. However, it is clear from this $\Delta P_{ml}(x)$ that nimodipine more closely approximates a true isomorph (i.e., there is a single, large difference between the drug-containing and control bilayer structures). The electron density increase attributed to the presence of nimodipine would then be located at ~14 Å from the methyl-trough.

Bretylium is a special case which is not adequately described by our simple model. Close examination of the electron density profiles of Fig. 4 *c* reveals that there is a slight shift in the headgroup position in the drug-containing bilayer, as well as, a broadening of this

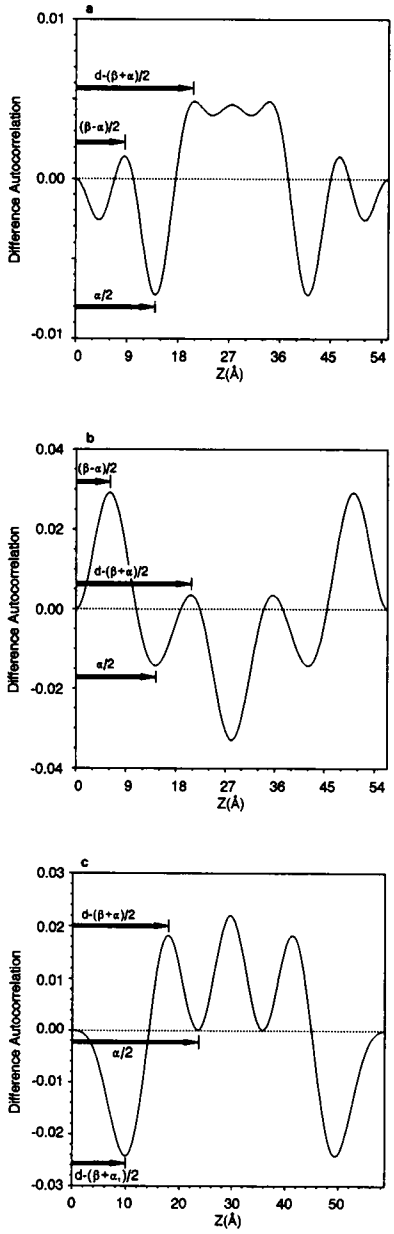

FIGURE 6 (*a*) The difference-autocorrelation function for the control versus clofilium-containing BCPC bilayers. The arrows indicate the origin of the autocorrelation (i.e., maxima and minima) in the $\Delta P_{ml}(x)$. The autocorrelations at 4 Å and $d/2$ arise from a perturbation near the water space. The α autocorrelation is predictably negligible, and not seen (see Appendix). The interpretation of this $\Delta P_{ml}(x)$ indicates $\alpha/2$ to be approximately 14 Å (i.e., the drug location is ~ ±14 Å from the bilayer center). (*b*) The difference-autocorrelation function for the control versus nimodipine-containing BCPC bilayers. The interpretatoin of these autocorrelations is shown in Fig. 5. The interpretation of this $\Delta P_{ml}(x)$ indicates $\alpha/2$ to be approximately 14 Å. (*c*) The difference-autocorrelation function for the control versus bretylium-containing BCPC bilayers. α and α_1 are defined in Fig. 4 *c*. Note that the autocorrelation at $d - (\beta + \alpha_1)/2$ is negative due to the electron-deficient perturbation represented by α_1. The apparent maximum at $d/2$ arises from the overlap of the minima at $\alpha/2$ and $d - \alpha/2$, based on model calculations. The interpretation of this $\Delta P_{ml}(x)$ indicates $\alpha/2$ to be ~23 Å.

feature. This results in a decrease in electron density near the edge of the unit cell and an increase in electron density adjacent to the headgroup as observed in the $\Delta\rho(x)$. Thus far, our working definition of an isomorph has been a single significant perturbation in bilayer structure between a control and drug-containing bilayer. In the case of bretylium, there are two such perturbations. Our model can be extended to accommodate two perturbations in the bilayer structure.

The $\Delta P_{ml}(x)$, calculated for the bretylium versus control $P_{ml,N}(x)s$, (Fig. 6 *c*) indicated a minimum at 10 Å, a maximum at 18 Å and a second minimum at 23 Å. Given the model described above, the minimum at 10 Å arises from the autocorrelation of the electron-deficient perturbation with the nearest headgroup in the adjacent unit cell of the multibilayer. The maximum at 18 Å then arises from the autocorrelation of the electron-dense perturbation with the nearest headgroup in the adjacent unit cell. The final minimum at 23 Å arises from the autocorrelation of the electron-dense perturbation with the methyl trough. This interpretation is consistent with the observed $\Delta P_{ml}(x)$ and is a reasonable interpretation of the electron density profiles. The electron density increase attributed to the presence of bretylium would then be located approximately 23 Å from the methyl-trough, within the headgroup region of the bilayer structure.

DISCUSSION

Methodological approach

We have identified the location of a typical DHP and two Class III antiarrhythmic agents in reconstituted bovine cardiac phosphatidylcholine membranes. The traditional approach used in membrane diffraction to answer similar questions is to phase the diffraction data by swelling and to calculate electron density profiles. These electron density profiles are then "scaled" and "offset" relative to one another based on some physical chemical property of the system being studied. It is assumed that the correct scale factors and offsets are found when some feature between profiles superimposes, such as the methyl trough or headgroup regions. This can be a reasonable assumption if one, a priori, has knowledge of some physical property of the membrane system being studied.

The methods we introduce in this paper allow us to ascertain the location of perturbations to bilayer structures, in this case attributed to the incorporation of drug molecules into biological membranes. Our method is consistent with traditional methods in that $F(0)$ is assumed to be zero. We introduce a scale factor in demanding the autocorrelation function to be unity at the origin. The effect of this normalization factor is calculated in the Appendix and will be discussed in a future paper. These are reasonable assumptions if we consider the drug molecules (in the concentrations used) to be a small perturbant. An advantage of this approach is that the difference-autocorrelation function is phase independent. Although this did not help much in our case, demanding consistency between $\Delta P_{ml}(x)$ and $\Delta\rho(x)$ can be used for phase determination. Our interpretation of the difference-autocorrelation functions requires a predetermined knowledge that we have a multibilayer structure and that we have the isomorphous addition of drug molecules to this structure.

Even for a single perturbation, the analysis can be complex (see Appendix). As we increase the number of perturbations, the number of terms we must reconcile increases quadratically. With this consideration in mind, we anticipate developing a pattern-recognition approach to aid us in interpreting the difference-autocorrelation functions. The pattern-recognition would be based on the relative positions, magnitudes and distributions of the autocorrelations arising from specific perturbations. The patterns would be derived from model calculations where the contribution of each feature is well defined.

The method described in this paper allows us to overcome some of the limitations introduced by arbitrary scaling and offsetting of relative electron density profiles. We are able to determine with reasonable certainty the location of the perturbation, and we demand our difference-electron density profiles to be consistent with this interpretation. We are thus able to place our electron density profiles on relative absolute scales.

Molecular model

To further investigate DHP interactions with biological membranes, we have investigated the ability of Class III antiarrhythmic agents to nonspecifically inhibit DHP-receptor binding in cardiac sarcolemmal membranes. The low receptor site density in cardiac sarcolemma (McCloskey and Poo, 1986) and the high affinity of DHPs for the membrane bilayer (Herbette et al., 1986) makes the "membrane bilayer pathway" an attractive hypothesis for DHP-receptor interactions. The partitioning of DHPs into membrane bilayers has been considered to be a nonspecific binding to a discrete level within the anisotropic environment of the membrane bilayer, which then potentiates drug binding to its high affinity receptor site. A further extension of this theory is that other amphiphilic drugs can nonspecifically inhibit DHP binding to its receptor site by drug–drug interactions

within the membrane, by virtue of their membrane localization.

This study arose from the observation that two structurally related drugs behave differently as inhibitors of DHP binding to the calcium channel receptor in cardiac membranes. In contrast to bretylium, clofilium nonspecifically inhibits nimodipine binding to its receptor site in cardiac sarcolemmal membranes. An inhibition constant of $K_i \simeq 5$ μM was observed for clofilium competed against nimodipine for receptor binding (similar results were observed with amiodarone competed against nimodipine). Because clofilium can inhibit nimodipine binding but itself does not bind to the DHP high affinity receptor site, the nonspecific interaction of clofilium with nimodipine in the membrane bilayer appears to be the simplest explanation. Bretylium has emerged as an exception to many of these ligands in its partition and binding-inhibition properties, exemplified by comparison to clofilium and amiodarone. Bretylium is lipid and slightly water soluble, and would be expected to occupy a time-averaged location near to the hydrocarbon core/water interface. Clofilium, with its alkyl chains, would be expected to partition deeper into the hydrocarbon core region of the membrane bilayer, whereas amiodarone has been shown to occupy a location deep in the hydrocarbon core region of model membrane bilayers (Trumbore et al., 1988). The localization of these drugs in native membrane bilayers could then explain their inhibition properties.

The amphiphilic DHPs appear to interact primarily with the acyl chains of the bilayer hydrocarbon core, exemplified by the localization of nimodipine in BCPC bilayers. A large portion of the molecular mass of these compounds is located below the hydrocarbon core/water interface. The Class III antiarrhythmic amiodarone has been shown to inhibit nimodipine binding to sarcolemmal receptor sites (data not shown). Amiodarone has also previously been shown to occupy a location in the membrane bilayer spanning most of the hydrocarbon core region, thus, overlapping the location occupied by nimodipine. Because of the size of amiodarone and its membrane location, its ability to inhibit nimodipine binding could not be assigned to any specific chemical moiety of it's structure. Presently, it has been demonstrated that bretylium has no effect on DHP receptor binding, whereas the structurally related Class III antiarrhythmic clofilium has a marked effect. In the presence of bretylium, the electron density profile structures indicate additional electron density at ±19 Å from the bilayer center in the phospholipid headgroup region of the BCPC membrane bilayers. In the presence of clofilium, an increase in electron density was observed centered at ±13 Å from the bilayer center. Because the structure of these two drugs are dominated by their halogenated-phenyl rings, the two phenyl rings occupy different locations within the anisotropic membrane environment. In the presence of nimodipine, an increase in electron density was observed at ±16 Å, with an extent from 9 Å to 22 Å.

These results indicated that clofilium's and bretylium's phenyl rings occupied different locations in BCPC bilayers, and that these locations are enveloped by the location of nimodipine. This may explain the inhibition of nimodipine binding in CSL membranes. The distribution of increased electron density attributed to the presence of nimodipine completely superimposed the distributions of bretylium and clofilium. In addition, neutron diffraction of selectively deuterated analogs (2,6-methyl groups on the dihydropyridine ring) of nimodipine demonstrated that the dihydropyridine methyl-groups were located at the hydrocarbon core/water interface, with the phenyl-ring moiety, more than likely, positioned towards the center of the bilayer (Herbette, 1985).

Reexamining the structural formulas (Fig. 1), the charged-amine to phenyl-ring distance differs, between bretylium, and clofilium, by three methylene segments. Assuming the charged-amine to prefer the hydrocarbon core/water interfacial region of the bilayer, and the aryl-ring to prefer the hydrophobic environment of the acyl-chain region of the bilayer, we can calculate an estimated difference between the locations of the two drugs based on their physical properties. We can then directly compare this empirical calculation to the observed difference-electron density profiles. Based on this orientation, and the average length of a carbon-carbon bond (1.54 Å), the positions of the two phenyl-moieties in the bilayer would be expected to differ by 4.6 Å. The experimentally determined difference is actually 6 Å, which is reasonably close to our calculation considering experimental error, the fluid nature of the BCPC bilayers, and the time-averaged distribution observed for these drugs.

In light of this, the inhibition of nimodipine's binding to its receptor by clofilium would seem to arise from the interaction of clofilium's phenyl ring with nimodipine's phenyl ring at the same membrane bilayer location. Bretylium's phenyl ring would then interact at the same membrane bilayer location of nimodipine's dihydropyridine moiety. Therefore, DHP-receptor site interactions would appear to require localization of the DHP in the hydrocarbon chain region of the bilayer. The proposed model is a reasonable interpretation which takes into account all of the experimental information (Fig. 7). Mechanistically, the nonspecific inhibition could then originate from either (*a*) interference with DHP localiza-

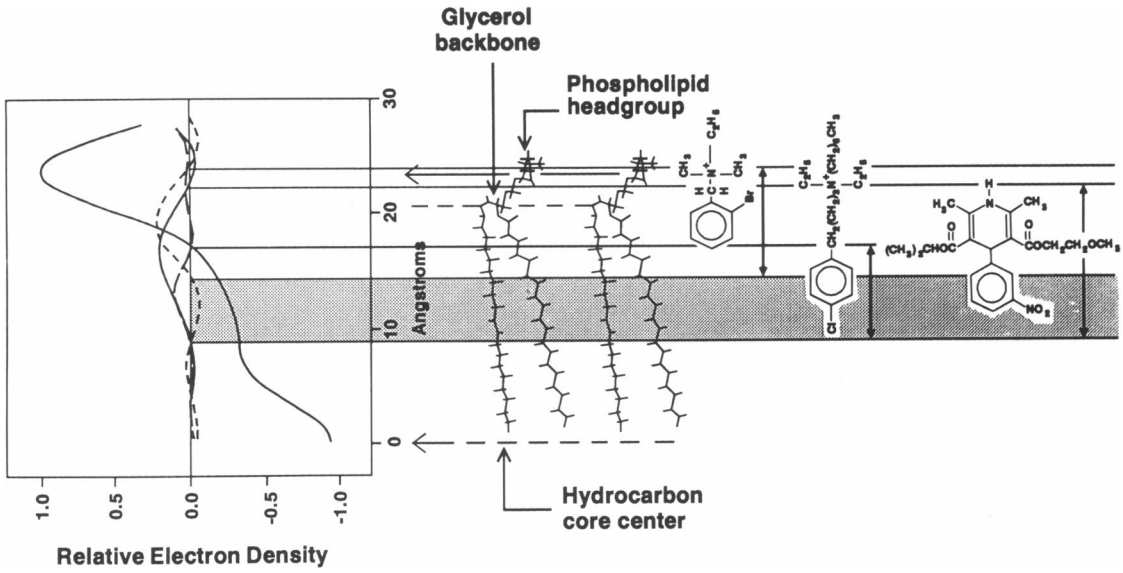

FIGURE 7 Molecular model. The combined diffraction and competition binding results are consistent with the schematic model illustrated above. The nonspecific inhibition phenomenon is a steric effect of one amphiphile upon another. The halogenated-phenyl ring of bretylium is located in the head group region of the BCPC membrane, whereas that of clofilium is located within the acyl-chain region of the bilayer. The charged amine of both drugs is expected to remain associated with the hydrocarbon core/water interface. Nimodipine spans both of these regions, presumably with the pyridine ring oriented such that the methyl-groups align at the hydrocarbon core/water interface (Herbette, 1985) and the phenyl ring extends into the acyl-chain region of the BCPC bilayer. Within the limits of the "membrane bilayer pathway" proposed by Rhodes et al. (1985), the functional location for DHP-receptor binding is that occupied by clofilium, within the bulk lipid phase (indicated by the shaded region).

tion and/or lateral diffusion preventing the specific DHP-protein receptor site interaction, presumably initiated by the phenyl-ring portion of nimodipine (a bulk lipid bilayer effect), or (*b*) the phenyl ring of clofilium could sterically inhibit the movement of the phenyl ring of nimodipine from its location in the lipid annulus to the calcium channel receptor site (a lipid annulus/protein interface effect), or (*c*) the inhibition could occur directly at the calcium channel receptor by the nonspecific interaction of clofilium's phenyl ring with the protein receptor site, thereby inhibiting the specific binding of nimodipine (a protein receptor site effect). The first possible mechanism is unlikely given the low concentrations of drugs used in the binding studies. The second mechanism is intriguing because it implies that the receptor site includes low affinity anchoring in the lipid annulus, with high affinity interactions confined to the protein receptor, and that the two interactions may be coupled. The third mechanism is analogous to the second in that first, a low affinity anchoring of clofilium's phenyl ring to the protein receptor site occurs, thereby inhibiting the interaction of nimodipine's phenyl ring with the receptor. According to this model, clofilium does not go on to bind with high affinity to the DHP receptor, presumably because it lacks the necessary chemical structure of the dihydropyridine ring.

CONCLUSION

Static model

These studies are consistent with the "membrane bilayer pathway" for DHP-receptor binding proposed by Rhodes et al. (1985). The results presented above support the access of nimodipine to its receptor site, in cardiac sarcolemmal membranes, via the acyl-chain region of the bilayer. Because nimodipine typifies the class of DHP calcium channel antagonists, these results strongly support the membrane bilayer pathway as a general mechanism of DHP-receptor interaction. The differential ability of bretylium and clofilium to nonspecifically inhibit nimodipine-receptor binding in CSL membranes suggests that this inhibition arises from the steric interaction of clofilium's phenyl ring with nimodipine's phenyl ring in either the membrane bilayer, lipid annulus or protein receptor site at a specific location in the membrane bilayer. This would then implicate the phenyl-ring portion of nimodipine as an initiating recognition element for binding to the calcium channel receptor site in addition to its probable role of orienting and anchoring the DHP within the membrane bilayer to set up a site specific interaction of nimodipine's dihydropyridine ring with its receptor.

Dynamic model

The static location information obtained from the small angle x-ray diffraction studies has been extrapolated to the nonspecific inhibition of DHP-receptor binding. The time-averaged locations are representative of the rapid partitioning and localization of the drugs in canine cardiac sarcolemmal membranes. These locations should then reflect the kinetic events responsible for the inhibition of nimodipine binding. The final state of equilibrium must be independent of the pathway. However, if the receptor site is considered to have specific and nonspecific components as a result of lipid and/or protein, inhibition of the nonspecific binding component could alter the final state of equilibrium. Alternatively, the phenyl-ring of clofilium could sterically inhibit the phenyl ring of nimodipine from binding at the calcium channel receptor site.

APPENDIX

To a first approximation, we can describe the electron density profile for the lipid bilayer by the following equation:

$$\rho_1(x) = g_1 * \left[\delta\left(-\frac{\beta}{2}\right) + \delta\left(\frac{\beta}{2}\right)\right] + g_2 * \delta(0), \quad (1)$$

where g_1 and g_2 are Gaussian distributions centered around the origin, i.e.,

$$g_n = A_n \exp(-\pi\omega_n^2 x^2)$$

with

$$\omega^2 = \frac{4ln2}{(FWHM)^2\pi}.$$

For our model $A_2 < 0 < A_1$ and β is the separation between the headgroup regions. The methyl trough region is centered at zero. The "*" denotes the convolution product, and "δ" the Dirac delta function. The unit cell autocorrelation, $P(x)$, is given by

$$P(x) = \rho(x) * \rho(-x). \quad (2)$$

If the bilayers are stacked into multibilayers, with a bilayer periodicity of d, then the multibilayer autocorrelation, P_{ml} is given by

$$P_{ml}(x) = P(x) + P(d - x), \quad (3)$$

For $0 < x < d$. Eq. 3 is sufficient to reconstruct the multilayer autocorrelation function everywhere because the function is periodic in d. It is also centrosymmetric around $(2n + 1)d/2$, where n is an integer.

If we assume a perturbation or isomorph to be described by a Gaussian distribution, g_3, located at $\pm\alpha/2$ from the bilayer center, the electron density profile for the isomorph is given by

$$\rho_2(x) = \rho_1(x) + g_3 * \left[\delta\left(-\frac{\alpha}{2}\right) + \delta\left(\frac{\alpha}{2}\right)\right]. \quad (4)$$

Given Eqs. 1–4, we can calculate for $0 < x < d$,

$$\begin{aligned}\Delta P_{ml} &= P_{ml,N_2}(x) - P_{ml,N_1}(x)\\ &= \left[\frac{\tilde{g}_1^2}{2\tilde{g}_1^2(0) + \tilde{g}_2^2(0) + 2\tilde{g}_3^2(0)} - \frac{\tilde{g}_1^2}{2\tilde{g}_1^2(0) + \tilde{g}_2^2(0)}\right]\\ &\quad * [\delta(\beta) + \delta(d - \beta)]\\ &\quad + \left[\frac{2g_1 * g_2}{2\tilde{g}_1^2(0) + \tilde{g}_2^2(0) + 2\tilde{g}_3^2(0)} - \frac{2g_1 * g_2}{2\tilde{g}_1^2(0) + \tilde{g}_2^2(0)}\right]\\ &\quad * \left[\delta\left(\frac{\beta}{2}\right) + \delta\left(d - \frac{\beta}{2}\right)\right] + \left[\frac{2g_1 * g_3}{2\tilde{g}_1^2(0) + \tilde{g}_2^2(0) + 2\tilde{g}_3^2(0)}\right]\\ &\quad * \left[\delta\left(\frac{\beta + \alpha}{2}\right) + \delta\left(\frac{\beta - \alpha}{2}\right)\right.\\ &\quad \left. + \delta\left(d - \frac{\beta + \alpha}{2}\right) + \delta\left(d - \frac{\beta - \alpha}{2}\right)\right]\\ &\quad + \left[\frac{2g_2 * g_3}{2\tilde{g}_1^2(0) + \tilde{g}_2^2(0) + 2\tilde{g}_3^2(0)}\right] * \left[\delta\left(\frac{\alpha}{2}\right) + \delta\left(d - \frac{\alpha}{2}\right)\right]\\ &\quad + \left[\frac{\tilde{g}_3^2}{2\tilde{g}_1^2(0) + \tilde{g}_2^2(0) + 2\tilde{g}_3^2(0)}\right] * [\delta(\alpha) + \delta(d - \alpha)]. \quad (5)\end{aligned}$$

where $\tilde{g}_n^2 = g_n * g_n$ and $P_{ml,N}(x) = P_{ml}(x)/\eta$. η is a normalization constant derived from the weighting of the $\delta(0)$ term in Eq. 3. A consequence of normalization is to remove any scaling bias in the data. Eq. 5 is valid for $0 < \alpha < \beta < d$. For $0 < \beta < \alpha < d$, $(\beta - \alpha)$ is replaced by $(\alpha - \beta)$ in Eq. 5, everywhere.

The major contributions to $\Delta P_{ml}(x)$ are at $(\beta + \alpha)/2$, $(\beta - \alpha)/2$, $d - (\beta + \alpha)/2$, $d - (\beta - \alpha)/2$, $\alpha/2$ and $d - \alpha/2$ (for example, see Figs. 5 and 6 *b*). Terms at α and $d - \alpha$ are small because $\tilde{g}_3^2 \ll \tilde{g}_1^2$ or $\tilde{g}_2^2$. $\beta/2$, $d - \beta/2$, β and $d - \beta$ arise from normalization and are predicted to be small for the same reason.

This formalism can be extended to include multiple perturbations and to accommodate situations where three or more Gaussians are required to model the electron density profile of the lipid bilayer in Eq. 1. These and other considerations will be specifically addressed in a future manuscript.

We would like to thank Dr. David Chester for his initial input in the autocorrelation analysis and continual discussions regarding the physical chemistry of lipids. We would like to thank American Hospital Supply Corporation and Eli Lily and Company for generously providing us with bretylium and clofilium. We would especially like to thank Ms. Yvonne Vant Erve for her technical assistance in competition binding analyses.

This project was primarily supported by a research grant from the National Institutes of Health (HL-33026), the American Heart Association, the American Health Assistance Foundation, and with support from Miles Pharmaceuticals, West Haven, CT. H.S. Young was supported by a Health Center Research Advisory Committee graduate student fellowship. L.G. Herbette was an Established Investigator of the American Heart Association. V. Skita was supported by a American Lung Association Research Grant and the National Institutes of Health (HL-45284). R.P. Mason was supported by an American Heart Association postdoctoral fellowship. The Biomolecular Structure Analysis Center acknowledges support from R.J.R. Nabisco Incorporated, the Patterson Trust Foundation, and the State of Connecticut Department of Higher Education's High Technology Programs.

Received for publication 25 June 1990 and in final form 26 August 1991.

REFERENCES

Affolter, H., and R. Coronado. 1985. Agonists of Bay K 8644 and CGP 28392 open channels from skeletal muscle transverse tubules. *Biophys. J.* 48:341–347.

Bangham, A. D., M. M. Standish, and J. C. Watkins. 1965. Diffusion of univalent ions across the lamellae of swollen phospholipids. *J. Mol. Biol.* 13:238–252.

Belleman, P., A. Schade, and R. Towart. 1983. Dihydropyridine receptor in rat brain labeled with [^{3}H] nimodipine. *Proc. Natl. Acad. Sci. USA.* 80:2356–2360.

Chester, D. W., L. G. Herbette, R. P. Mason, A. F. Joslyn, D. J. Triggle, and D. E. Koppel. 1987. Diffusion of dihydropyridine calcium channel antagonists in cardiac sarcolemmal lipid multibilayers. *Biophys. J.* 52:1021–1030.

Franks, N. P., and W. R. Lieb. 1987. What is the molecular nature of general anesthetic target sites? *TIPS (Trends Pharmacol. Sci.).* 8:109–114.

Herbette, L. G. 1985. X-ray and neutron diffraction for probing the interactions of small molecules with biological membrane structures. *Curr. Topics Bioenergetics.* 14:21–52.

Herbette, L. G., D. W. Chester, and D. G. Rhodes. 1986. Structural analysis of drug molecules in biological membranes. *Biophys. J.* 49:91–94.

Herbette, L. G., T. MacAlister, T. F. Ashavaid, and R. A. Colvin. 1985. Structure-function studies of canine cardiac sarcolemmal membranes. II. Structural organization of the sarcolemmal membranes as determined by electron microscopy and lamellar x-ray diffraction. *Biochim. Biophys. Acta.* 812:609–623.

Herbette, L. G., D. G. Rhodes, and R. P. Mason. 1991. New approaches to drug design and delivery based on drug-membrane interactions. *Drug Design and Delivery.* 7:75–118.

Hille, B. 1977. Local anesthetics: Hydrophilic and hydrophobic pathways for the drug-receptor reaction. *J. Gen. Physiol.* 69:497–515.

Janis, R. A., P. J. Silver, and D. J. Triggle. 1987. Drug action and cellular calcium regulation. *Adv. Drug Res.* 16:309–591.

Jones, L. R., S. W. Maddock, and H. R. Besch. 1980. Unmasking effects of almethacin on the Na/K ATPase, β-adrenergic receptor-coupled adenylate cyclase and cAMP-dependent protein kinase activities in cardiac sarcolemmal vesicles. *J. Biol. Chem.* 255:9971–9980.

Kokubun, S., and H. Reuter. 1984. Dihydropyridine derivatives prolong the open state of Ca^{++} channels in cultured cardiac cells. *Proc. Natl. Acad. Sci. USA.* 81:4824–4827.

Martin, B. R. 1986. Cellular effects of cannabinoids. *Pharmacol. Rev.* 38:45–74.

Mason, R. P., J. Moring, and L. G. Herbette. 1990. A molecular model involving the membrane bilayer in the binding of lipid soluble drugs to their receptors in heart and brain. *Nucl. Med. Biol.* 17:13–33.

Mason, R. P., G. F. Gonye, D. W. Chester, and L. G. Herbette. 1989. Partitioning and location of Bay K 8644, 1,4-dihydropyridine calcium channel agonist, in model and biological membranes. *Biophys. J.* 55:769–778.

McCloskey, M., and M. M. Poo. 1986. Rates of membrane associated reaction: reduction of dimensionality revisited. *J. Cell Biol.* 102:88–96.

Miller, K. W., S. H. Roth. 1986. Inside the "black box." *In* Molecular and Cellular Mechanisms of Anesthetics. S. H. Roth, and K. W. Miller, editors. Plenum Publishing Corp., New York. 261–266.

Moody, M. F., 1963. X-ray diffraction of nerve myelin: a method for determining the phases. *Science (Wash. DC).* 142:1173–1174.

Rhodes, D. G., J. G. Sarmiento, and L. G. Herbette. 1985. Kinetics of binding of membrane-active drugs to receptor sites. Diffusion limited rates for a membrane bilayer approach of 1,4-dihydropyridine calcium channel antagonists to their active site. *Mol. Pharmacol.* 27:612–623.

Sayre, D. 1953. Some implications of a theorem due to Shannon. *Acta. Cryst.* 5:843.

Shannon, C. E. 1949. Communications in the presence of noise. *Proc. Inst. Radio Eng. N.Y.*

Steinberg, M. I. 1988. Electrophysiological effects of Class III antiarrhythmic agents in vitro and in vivo. *In* 21st National Medical Chemistry Symposium. Medicinal Chemistry Division, American Chemical Society.

Trumbore, M. W., D. W. Chester, J. Moring, D. Rhodes, and L. G. Herbette. 1988. Structure and location of amiodarone in a membrane bilayer as determined by molecular mechanics and quantitative x-ray diffraction. *Biophys. J.* 54:535–543.

Valdivia, H., and R. Coronado. 1988. Pharmacological profile of skeletal muscle calcium channel in planar lipid bilayers. *Biophys. J.* 53:555*a* (Abstr.)